

Event Voxel Set Transformer for Spatiotemporal Representation Learning on Event Streams

Bochen Xie, *Graduate Student Member, IEEE*, Yongjian Deng, *Member, IEEE*, Zhanpeng Shao, *Member, IEEE*, Hai Liu, *Senior Member, IEEE*, Qingsong Xu, *Senior Member, IEEE*, Youfu Li*, *Fellow, IEEE*

Abstract—Event cameras are neuromorphic vision sensors representing visual information as sparse and asynchronous event streams. Most state-of-the-art event-based methods project events into dense frames and process them with conventional learning models. However, these approaches sacrifice the sparsity and high temporal resolution of event data, resulting in a large model size and high computational complexity. To fit the sparse nature of events and sufficiently explore the relationship between them, we develop a novel attention-aware model named Event Voxel Set Transformer (EVSTr) for spatiotemporal representation learning on event streams. It first converts the event stream into voxel sets and then hierarchically aggregates voxel features to obtain robust representations. The core of EVSTr is an event voxel transformer encoder to extract discriminative spatiotemporal features, which consists of two well-designed components, including a Multi-Scale Neighbor Embedding Layer (MNEL) for local information aggregation and a Voxel Self-Attention Layer (VSAL) for global feature interactions. Enabling the network to incorporate a long-range temporal structure, we introduce a segment modeling strategy to learn motion patterns from a sequence of segmented voxel sets. We evaluate the proposed model on two event-based recognition tasks: object classification and action recognition. Comprehensive experiments show that EVSTr achieves state-of-the-art performance while maintaining low model complexity. Additionally, we present a new dataset (NeuroHAR) recorded in challenging visual scenarios to complement the lack of real-world event-based datasets for action recognition.

Index Terms—Event camera, neuromorphic vision, attention mechanism, object classification, action recognition.

I. INTRODUCTION

WITH the rapid development of neuromorphic vision sensors [1]–[3], event-based vision has broad and growing applications, including object classification [4]–[12], action recognition [13]–[16], and object detection [17]–[19]. The event camera measures per-pixel brightness changes asynchronously and acquires visual information as a stream of events. The events are sparsely and non-redundantly distributed in the x - y - t space, as shown in Fig. 1 (a). An event

Bochen Xie and Youfu Li are with the Department of Mechanical Engineering, City University of Hong Kong, Hong Kong SAR, China (e-mail: boxie4-c@my.cityu.edu.hk; meyfli@cityu.edu.hk).

Yongjian Deng is with the College of Computer Science, Beijing University of Technology, Beijing 100124, China (e-mail: yjdeng@bjut.edu.cn).

Zhanpeng Shao is with the College of Information Science and Engineering, Hunan Normal University, Changsha 410081, China (e-mail: zp-shao@hunnu.edu.cn).

Hai Liu is with the National Engineering Research Center for E-Learning, Central China Normal University, Wuhan 430079, China (e-mail: hailiu0204@mail.ccnu.edu.cn).

Qingsong Xu is with the Department of Electromechanical Engineering, University of Macau, Macao SAR, China (e-mail: qsxu@um.edu.mo).

*Corresponding author

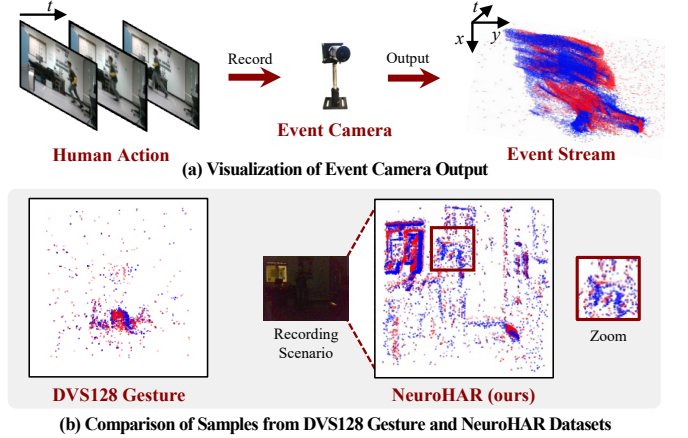


Fig. 1. (a) Visualization of event camera output. An event camera records the spatiotemporal information of the sample *running* as a stream of events, where red and blue dots denote positive and negative, respectively. (b) Comparison of samples from DVS128 Gesture and NeuroHAR datasets. The instance is a human action *hand clap*. After introducing handheld mobile recording, these samples in our proposed NeuroHAR contain both movement subject (zoom box) and background information. Besides, recording in the low-light illumination unlocks the high dynamic range advantage of event cameras.

encodes the spatial location, timestamp, and polarity of the brightness change for a pixel. Compared to traditional cameras with a fixed frame rate, event cameras can offer significant advantages in the following respects: low power consumption, high temporal resolution (in the order of μ s), and high dynamic range (> 120 dB) [20]. Thanks to these outstanding properties, the event camera unlocks great potential for recognition tasks in challenging visual scenarios (i.e., low-light illumination and high-speed movement). However, tailoring models for event streams with the specific data format remains challenging.

Existing event-based learning models can be summarized into two main categories: frame-based and point-based methods. Frame-based methods [4], [5], [7], [8] first convert events into dense frame-based representations and then process them using learning models designed for standard images, such as convolutional neural networks (CNNs) and vision transformers. Combined with the models pre-trained on large-scale image datasets (e.g., ImageNet [21]), frame-based methods achieve state-of-the-art performance on recognition tasks. However, the sparse-to-dense conversion sacrifices the sparse and asynchronous nature of event data, resulting in wasteful computation and high latency. To address this issue, point-based methods fit with the nature of events and achieve a trade-off between computational cost and accuracy. These

approaches treat a single event or a set of regional events as the basic unit and represent event streams as spikes [16], [22], 3D point clouds [14], [23], or graphs [9]–[11], [15], [19]. Event-based graph approaches achieve outstanding performance by learning geometric features on point-wise or voxel-wise graphs constructed from event streams. A key challenge of this line is how to model the spatiotemporal relationship between events for feature representation, but existing models have the following limitations. (i) The voxel-wise graph approaches [10], [11] only relies on geometric relationship to aggregate neighbor features. The aggregation procedure without considering semantic relations may fail to capture robust local information. (ii) Current approaches lack long-range feature interactions with the input, limiting the capability in learning global representations.

To address the above limitations, this work proposes a powerful yet lightweight model named Event Voxel Set Transformer (EVSTr) for spatiotemporal representation learning on event data. It can flexibly process both short- and long-duration event streams for recognition tasks, such as object classification and action recognition. We adopt the event voxel set representation [10], [11] as input, which is robust to noise while maintaining the sparse structure. The core of EVSTr is the event voxel transformer encoder, a spatiotemporal relation learner driven by the attention mechanism. The encoder starts by aggregating input features into local representations using Multi-Scale Neighbor Embedding Layers (MNEL). The proposed MNEL layer solves the first limitation by jointly modeling positional and semantic relations between neighboring voxels into attention scores for multi-scale feature aggregation. To solve the second problem, the embedded features are fed into Voxel Self-Attention Layers (VSAL) to enhance global representation capabilities by calculating semantic correlations between voxels. Overall, the event voxel transformer encoder hierarchically aggregates voxel features to obtain robust representations. For object classification, we combine the encoder and classifier to process a single voxel set converted from the event stream. Furthermore, we extend the network with a segment modeling strategy to learn temporal dynamics for action recognition. Specifically, we spilt a long-duration event stream into a sequence of segmented voxel sets, and extract spatiotemporal features per segment by the encoder. Then a sequence of features is fed to a Stream-Segment Temporal Modeling Module (S²TM) for aggregating the temporal dynamics. The proposed EVSTr model achieves state-of-the-art accuracy on these two recognition tasks while holding low model complexity.

In this work, we also present a new event-based action recognition dataset named Neuromorphic Human Action Recognition (NeuroHAR) to alleviate the limitations of current benchmark datasets. Existing real-world action recognition datasets [13], [16] are captured under relatively simple recording conditions (i.e., sufficient illumination and static cameras) which cannot reflect the real application scenarios of event cameras, such as dark environment and dynamic background. To build a more challenging and practical benchmark, we collect NeuroHAR using an event camera and a RGB-D camera in challenging recording scenarios, including low-light

illumination and camera motion. An intuitive comparison of NeuroHAR and the widely used DVS128 Gesture dataset [13] is shown in Fig. 1 (b). NeuroHAR contains 1,584 instances with 18 classes of daily actions and 3 visual modalities.

The main contributions of this paper are summarized as follows:

- To utilize the sparse nature of events and model their relationship, we propose the EVSTr model for efficiently learning spatiotemporal representations on voxelized event streams.
- We propose the event voxel transformer encoder with well-designed MNEL and VSAL layers to hierarchically learn and extract spatiotemporal features. Besides, the segment modeling strategy combined with S²TM endows our model with representation capabilities for long-range temporal modeling.
- We present a new event-based action recognition dataset (NeuroHAR). Challenging recording conditions enable it to provide convincing model evaluation.
- We evaluate the proposed model on object classification and action recognition tasks. Extensive experiments demonstrate it is superior to the state-of-the-art methods and has a significant advantage in model complexity.

II. RELATED WORK

A. Deep Learning on Event Streams

From the perspective of input representations, existing event-based learning models can be summarized into two mainstream strategies: frame-based and point-based methods.

1) *Frame-Based Methods*: This line of work first converts events within a time interval into dense frames and then processes them using off-the-shelf learning models tailored for standard images. Frame-based methods mainly focus on designing suitable representations to integrate the spatial semantics embedded in event streams. An example event frame is visualized in Fig. 2 (a). Some early works project events along the time-axis through handcrafted integration ways, such as cumulative quantity [24] and timestamp integration [25]. Then two learnable representations [4], [5] replace the handcrafted integration kernels with trainable ones to achieve better generalization on different vision tasks. Besides, some works improve the robustness of frame-based representations from other perspectives, such as motion-agnostic filter [7], multi-view integration [8]. Combined with pre-trained models, the frame-based family achieves state-of-the-art performance on many event-based tasks. To benefit from large-scale image datasets, the researchers design transfer learning schemes by leveraging knowledge from images to facilitate the training of event-based models, such as knowledge distillation [26], [27] and domain adaptation [28].

The conversion from events to dense frames sacrifices the sparse and asynchronous nature of events. Although frame-based methods outperform point-based ones in terms of accuracy, they usually require heavy-weight models to process dense input, leading to high computational complexity and latency. Some sparse frame-based solutions [6], [12] are proposed to tackle these limitations. They lag behind dense peers

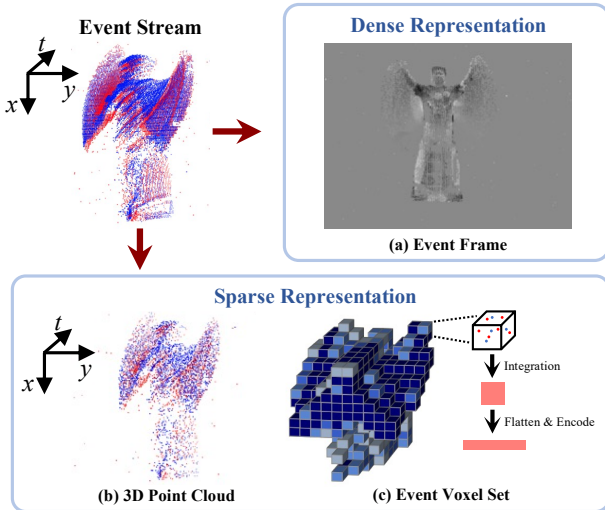


Fig. 2. Visualization of the human action *jumping jacks* with representative event-based representations. (a) Event frame. (b) 3D point cloud. (c) Event voxel set. The color of voxels from light to dark denotes the event density from small to large.

in accuracy and still cannot lead point-based methods in model complexity.

2) *Point-Based Methods*: Unlike frame-based counterparts, point-based methods exploit the sparsity and asynchrony of event data while achieving a good trade-off between accuracy and model complexity. They design sparse representations to convey the spatial and temporal information of event streams, as shown in Fig. 2 (b) and (c). A natural approach is to take events as input spikes and process them with spiking neural networks (SNNs) [16], [22] because the bio-inspired working mechanism of event cameras and SNNs is compatible [20]. While training an SNN is more intractable than other learning architectures (e.g., CNNs) due to the lack of efficient optimization methods [19]. Inspired by 3D point cloud processing, some researchers adopt the event-specific variants of PointNet [29] or PointNet++ [30] for several tasks, including semantic segmentation [23] and action recognition [14]. However, these network architectures have limited capabilities in capturing local features because they directly follow the point cloud processing manner, which does not fit the spatiotemporal structure of event data well.

Graph-based approaches [9], [15], [19] are proposed to address the issues by constructing point-wise graphs on the downsampled point set of event streams and exploiting graph neural networks (GNNs) for learning local representations better. Considering that the point-wise relationship of event data is susceptible to noisy signals, voxel-wise GNNs [10], [11] are proposed by first converting an event stream into a voxel set and then aggregating vertices' information for feature representation. The voxel-wise representation keeps more local semantics than the point-wise one, gaining the robustness to noise. As stated in Section I, current event-based GNNs still have many limitations needed to be improved. In this paper, we take the well-designed voxel-wise representation as input and introduce a novel learning model (EVSTr) based on attention

mechanism to improve event-based representation learning.

B. Transformers in Vision

The great success of transformer architectures [31] in natural language processing attracts increasing interest among computer vision researchers. The key component of transformer is the self-attention mechanism that computes semantic correlations between input elements to model long-range dependencies. Researchers have recently applied transformer to many vision tasks, such as image recognition [32], [33], video classification [34]–[36], point cloud processing [37], [38], and event stream processing [12], [39]. Previous event-based self-attention networks take event frames as input and process them with vision transformers designed for images. Our interest is applying self-attention to the event voxel set representation for spatiotemporal feature learning. Inspired by point cloud transformer [37], we adopt the encoder design strategy from local to global modeling and propose a novel method with event-specific designs, such as multi-scale attentive aggregation for voxel-wise neighbor embedding and positional encoding for assisting self-attention to operate on spatiotemporal structures. Besides, we learn long-range temporal dynamics by the self-attention based segment modeling strategy for action recognition. Eventually, we develop the attention-aware EVSTr model with carefully designed transformer encoder and segment modeling strategy, which can correlate event voxel sets for efficiently learning spatiotemporal features.

III. METHODOLOGY

An overview of the proposed EVSTr model is illustrated in Fig. 3. It comprises four stages: event voxel set representation, spatiotemporal relation learning, long-range temporal modeling and classification. For object classification, an event stream is converted into a single event voxel set, whereas for action recognition on long-duration event streams with complex temporal structure, a sequence of segmented voxel sets are collected as input. Each event voxel set is processed by the event voxel transformer encoder, which extracts spatiotemporal features through learning inter-voxel relations. A single voxel set is modeled for object classification, and we feed its feature into a classifier for prediction. For action recognition, we first utilize a segment modeling strategy to learn temporal dependencies from the input sequence and then transform the final representation into action categories.

Section III-A introduces the event camera's working principle and event voxel set representation. The core components (MNEL and VSAL) of event voxel transformer encoder and the procedure of spatiotemporal relation learning are detailed in Section III-B. We introduce the long-range temporal modeling for action recognition in Section III-C. Finally, we detail the network architectures of our model applied to object classification and action recognition in Section III-D.

A. Event Voxel Set Representation

The event camera triggers an individual event $\mathbf{e}_i = \{x_i, y_i, t_i, p_i\}$ asynchronously when the logarithmic brightness

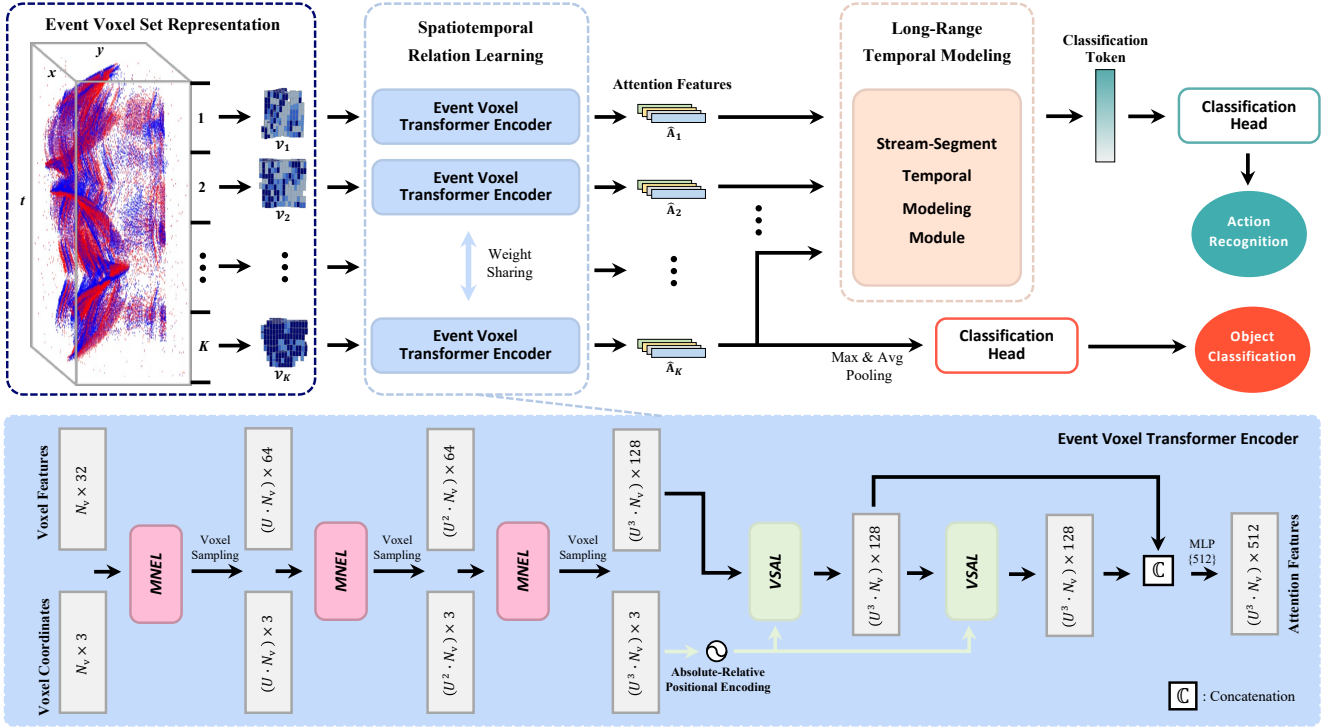


Fig. 3. The pipeline of the Event Voxel Set Transformer (EVSTr) model for spatiotemporal representation learning on event streams. Our model can be applied to both object classification and action recognition tasks. We construct a sequence of K segmented event voxel sets as input of EVSTr (where $K = 1$ for object classification). The event voxel transformer encoder propagates each event voxel set to extract spatiotemporal features. For object classification, we feed the encoder output into a classification head for predicting classes. For action recognition, we first model long-range temporal dynamics over multiple voxel sets by a Stream-Segment Temporal Modeling Module and then transform the class token’s feature into categories. N_v represents the number of input events voxels, and U denotes the downsampling rate of voxel sampling.

L at pixel (x_i, y_i) and time t_i changes by a certain threshold C ($C > 0$) [20]:

$$L(x_i, y_i, t_i) - L(x_i, y_i, t_i - \Delta t_i) = p \cdot C, \quad (1)$$

where Δt_i is the time interval between the last and current events at the same pixel, and $p_i \in \{+1, -1\}$ is the polarity of brightness change (+1 and -1 denote increasing and decreasing, respectively). An event can be treated as a point in 3D space, with a spatiotemporal coordinate $\{x_i, y_i, t_i\}$ and polarity attribute p_i .

As shown in Fig. 2 (c), we adopt the voxel-wise representation strategy [10], [11] to convert an event stream $\mathcal{E} = \{\mathbf{e}_i\}_N$ into a voxel set $\mathcal{V} = \{\{\mathbf{f}_i, \mathbf{c}_i\}\}_{N_v}$, where N and N_v are the number of events and voxels, respectively. Here, $\mathbf{f}_i \in \mathbb{R}^{D_f}$ and $\mathbf{c}_i = (x_i^c, y_i^c, t_i^c) \in \mathbb{R}^3$ are the feature and spatiotemporal coordinate of an event voxel. Specifically, we normalize the temporal dimension with a compensation coefficient T by $t_i^* = T \times (t_i - t_1) / (t_N - t_1)$. Given the spatial resolution of event camera as (H, W) , we first partition an event stream into voxels with a size of (H_v, W_v, T_v) and then use motion-sensitive voxel sampling [11] to select N_v representative ones. Assuming that a voxel contains M events $\{(x_j^v, y_j^v, t_j^v, p_j^v)\}_M$, we integrate these events into a 2D patch $\mathbf{F}_i \in \mathbb{R}^{H_v \times W_v}$ along the t -axis by

$$\mathbf{F}_i(x, y) = \sum_{j=1}^M p_j^v \cdot \delta(x - x_j^v, y - y_j^v) \cdot t_j^v, \quad (2)$$

where $\delta(\cdot)$ is the Dirac delta function. Then we flatten \mathbf{F}_i into a 1D vector in $\mathbb{R}^{H_v \cdot W_v}$ and use a multi-layer perceptron (MLP) for voxel feature encoding:

$$\mathbf{f}_i = \text{MLP}(\Gamma(\mathbf{F}_i)), \quad (3)$$

where $\Gamma(\cdot)$ is a flattening operation and $\text{MLP}(\cdot)$ consists of a linear layer, a batch normalization (BN) and a ReLU function. Eventually, we obtain the event voxel set representation \mathcal{V} not only retains local semantics inside voxels but also keeps the sparse structure of event data.

B. Spatiotemporal Relation Learning

The event voxel set is fed into the event voxel transformer encoder, where our model learns the spatiotemporal relations between input elements, as illustrated in Fig. 3. The encoder is endowed by two carefully designed components: Multi-Scale Neighbor Embedding Layer (MNEL) for local information embedding and Voxel Self-Attention Layer (VSAL) for global feature interactions. In the following, we successively detail their design strategies and how to build the encoder with them.

1) Multi-Scale Neighbor Embedding Layer: The MNEL layer jointly models positional and semantic relations into attention scores for adaptive feature aggregation. Moreover, a multi-scale embedding strategy is introduced to enhance the local representation on non-uniform input.

Given an event voxel set $\mathcal{V} = \{\{\mathbf{f}_i, \mathbf{c}_i\}\}_{N_e}$, the MNEL layer learns a local representation for each voxel by embedding

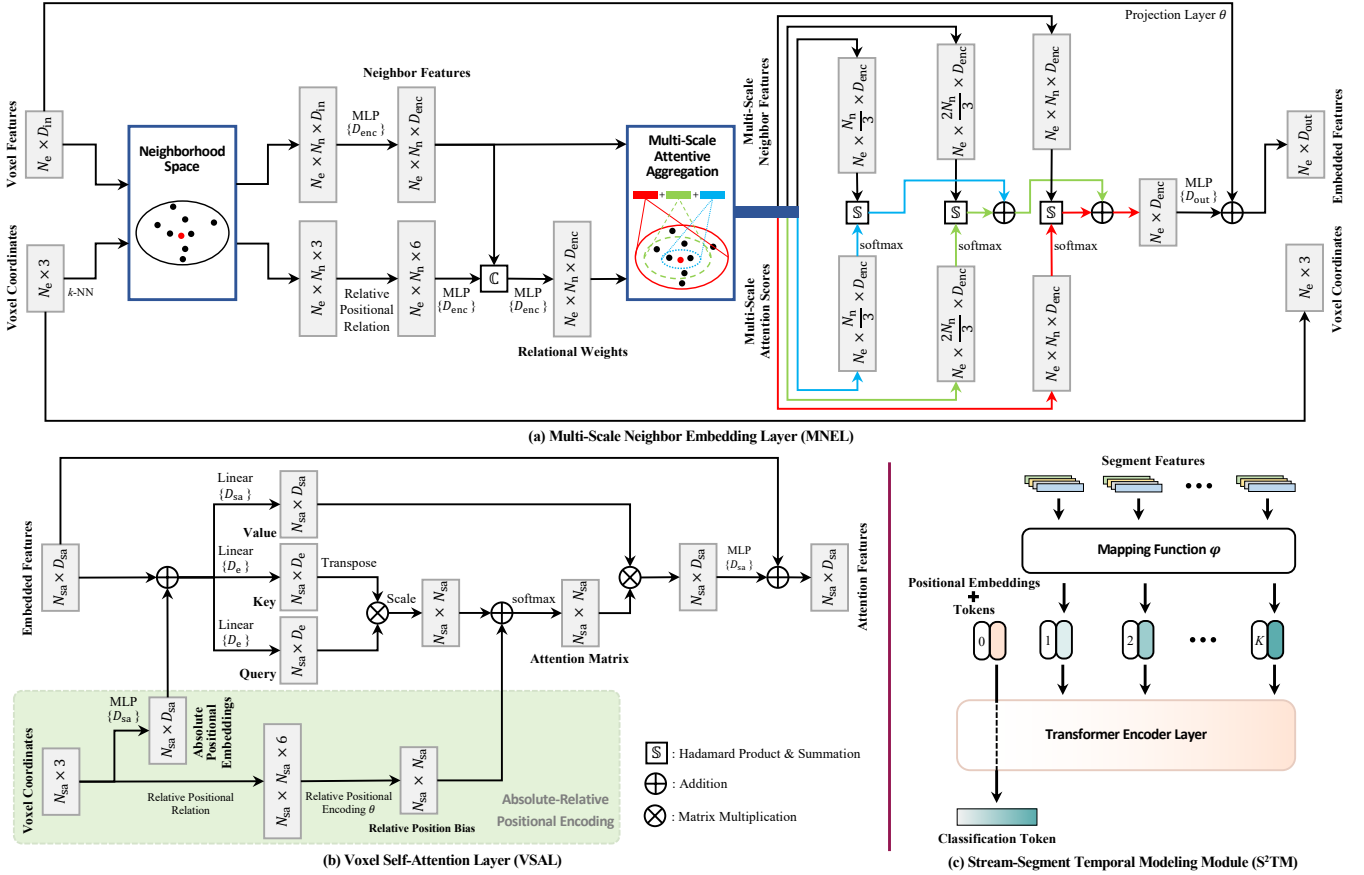


Fig. 4. The architecture of three components in the EVSTr model. (a) Multi-Scale Neighbor Embedding Layer (MNEL). It attentively aggregates multi-scale neighbor features into a local representation for each voxel. (b) Voxel Self-Attention Layer (VSAL). It models the feature interactions between voxels to enhance the global representation. We introduce the absolute-relative positional encoding for assisting the self-attention operator in fitting with the spatiotemporal structure. (c) Stream-Segment Temporal Modeling Module (S²TM). It is designed for action recognition by learning the long-range temporal dynamics from a sequence of segmented features.

multi-scale neighbor features. For the i th voxel, we gather its N_n neighboring voxels by the k -nearest neighbours (k -NN) algorithm based on the Euclidean distance of coordinates. This k -NN set includes self-loop which means the central voxel also links itself as a neighbor. In this neighborhood space, $\mathbf{f}_{ij} \in \mathbb{R}^{D_{in}}$ and $\mathbf{c}_{ij} \in \mathbb{R}^3$ indicate the feature and coordinate of the central voxel's j th neighbor respectively, where $j \in \{1, 2, \dots, N_n\}$. We define the relative positional relation of a neighboring pair as $\mathbf{r}_{ij} = \mathbb{C}(\mathbf{c}_i, (\mathbf{c}_i - \mathbf{c}_{ij})) \in \mathbb{R}^6$, where $\mathbb{C}(\cdot)$ is the concatenation operation. Then we encode the features and relative positional relations of N_n neighboring voxels with MLP layers individually as follows:

$$\tilde{\mathbf{f}}_{ij} = \text{MLP}(\mathbf{f}_{ij}) \in \mathbb{R}^{D_{enc}}, \quad \tilde{\mathbf{r}}_{ij} = \text{MLP}(\mathbf{r}_{ij}) \in \mathbb{R}^{D_{enc}}. \quad (4)$$

To represent an integrated relationship for each neighboring pair, we design a function to generate relational weights $\hat{\mathbf{r}}_{ij} \in \mathbb{R}^{D_{enc}}$ by fusing positional and semantic cues. The function is formally defined as follows:

$$\hat{\mathbf{r}}_{ij} = \text{MLP}(\mathbb{C}(\tilde{\mathbf{f}}_{ij}, \tilde{\mathbf{r}}_{ij})). \quad (5)$$

Thus, we obtain a k -NN set $\{(\tilde{\mathbf{f}}_{ij}, \hat{\mathbf{r}}_{ij})\}_{j=1}^{N_n}$ of neighbor features with corresponding relational weights. Inspired by PointNet++ [30], we propose a novel multi-scale attentive

aggregation strategy to enhance local feature extraction. According to the distance from the nearest neighbor to the central voxel, we divide the k -NN set into L subspaces of gradually increasing spatiotemporal scale. Our strategy combines aggregated features from multi-scale neighborhood subspaces to the central voxel as a joint one for robust representation. In each subspace, we transform relational weights into attention scores as a soft mask, adaptively re-weighting neighbor features for summation. The procedure of feature aggregation can be formalized as follows:

$$\hat{\mathbf{f}}_i = \text{MLP}\left(\sum_{l=1}^L \sum_{j=1}^{l \cdot N_n / L} \tilde{\mathbf{f}}_{ij} \odot \text{softmax}(\hat{\mathbf{r}}_{ij})\right), \quad (6)$$

where $\hat{\mathbf{f}}_i \in \mathbb{R}^{D_{out}}$ is a joint representation of the i th voxel embedded with multi-scale neighbor features, and the $\text{softmax}(\cdot)$ function is used to obtain multi-scale attention scores by translating per-subspace relational weights into probabilities. Here, \odot denotes Hadamard product. Finally, we use a shortcut connection to fuse the input and aggregated feature as output \mathbf{l}_i by

$$\mathbf{l}_i = \hat{\mathbf{f}}_i + \theta(\mathbf{f}_i), \quad (7)$$

where $\theta(\cdot)$ is a projection layer to guarantee that $\hat{\mathbf{f}}_i$ and \mathbf{f}_i have the same dimension. When D_{out} is equal to D_{in} , it is

an identity projection, otherwise it is an MLP to match the dimension. For efficiency, the number L of subspaces is 3 and we set D_{enc} to be $D_{\text{in}}/2$.

Finally, a new set of event voxels $\mathcal{N} = \{(\mathbf{l}_i, \mathbf{c}_i)\}_{N_e}$ is generated by the MNEL layer which attentively encodes a local representation embedded with multi-scale neighbor features for each voxel. After each MNEL layer, we utilize random sampling, a simple and efficient approach, to decrease voxel density and progressively enlarge the receptive field of feature aggregation. The downsampling rate of voxel sampling is a constant U . In the event voxel transformer encoder, we stack multiple MNEL layers and voxel sampling operations for hierarchically learning local representations and abstracting sets of event voxels.

2) **Voxel Self-Attention Layer:** After neighbor embedding by several MNEL layers, the encoder acquires the ability of local feature representation. We introduce a self-attention based VSAL layer to handle feature interactions between voxels. As illustrated in Fig. 4 (b), we adopt the self-attention operator from the original Transformer [31] and propose a positional encoding approach that allows the operator to adapt to the spatiotemporal structure of an event voxel set.

Formally, given an input $\mathcal{N} = \{(\mathbf{l}_i, \mathbf{c}_i)\}_{N_{\text{sa}}}$, VSAL calculates semantic affinities between voxels to learn a global representation $\tilde{\mathbf{A}} = \{\tilde{\mathbf{a}}_i\}_{N_{\text{sa}}}$, where $\tilde{\mathbf{a}}_i \in \mathbb{R}^{D_{\text{sa}}}$ is the attention feature of the i th voxel relating to all input features. We introduce a trainable absolute-relative positional encoding approach that can be embedded into the self-attention operator. Denoting that the input features are $\mathbf{L} = \{\mathbf{l}_i\}_{N_{\text{sa}}} \in \mathbb{R}^{N_{\text{sa}} \times D_{\text{sa}}}$ and spatiotemporal coordinates are $\mathbf{C} = \{\mathbf{c}_i\}_{N_{\text{sa}}} \in \mathbb{R}^{N_{\text{sa}} \times 3}$ in the set \mathcal{N} , we first add the absolute positional embeddings $\mathbf{P} \in \mathbb{R}^{N_{\text{sa}} \times D_{\text{sa}}}$ to \mathbf{L} and then map them into query (\mathbf{Q}), key (\mathbf{K}), and value (\mathbf{V}) matrices by linear transformations:

$$\mathbf{P} = \text{MLP}(\mathbf{C}), \quad (8)$$

$$(\mathbf{Q}, \mathbf{K}, \mathbf{V}) = (\mathbf{L} + \mathbf{P}) \cdot (\mathbf{W}_q, \mathbf{W}_k, \mathbf{W}_v), \quad (9)$$

where $\mathbf{Q}, \mathbf{K} \in \mathbb{R}^{N_{\text{sa}} \times D_e}$ and $\mathbf{V} \in \mathbb{R}^{N_{\text{sa}} \times D_{\text{sa}}}$. Here, $\mathbf{W}_q, \mathbf{W}_k \in \mathbb{R}^{D_{\text{sa}} \times D_e}$ and $\mathbf{W}_v \in \mathbb{R}^{D_{\text{sa}} \times D_{\text{sa}}}$ are the learnable weights of linear layers. For efficiency, we set D_e to be $D_{\text{sa}}/4$. Inspired by [33], we include a relative position bias $\mathbf{B} \in \mathbb{R}^{N_{\text{sa}} \times N_{\text{sa}}}$ to the scaled dot-product attention [31] in computing similarity. We calculate the relative positional relation for representing the relationship between any two voxels, and then design a encoding function to generate the bias matrix:

$$\mathbf{B}(i, j) = \phi(\mathbb{C}(\mathbf{c}_i, (\mathbf{c}_i - \mathbf{c}_j))), \quad (10)$$

where $i = \{1, 2, \dots, N_{\text{sa}}\}$ and $j = \{1, 2, \dots, N_{\text{sa}}\}$ denote the row and column index of \mathbf{B} respectively. Here, $\phi(\cdot)$ is a positional encoding function consisting of two linear layers separated by a BN layer and a ReLU function, which first projects the vector of relative positional relation into the dimension in \mathbb{R}^{N_e} and then squeezes it to a scalar. Eventually, we adopt the scaled dot-product attention equipped with the relative position bias to evolve the input set representation based on interactions among all its elements:

$$\mathbf{A} = \text{softmax}\left(\frac{\mathbf{Q} \cdot \mathbf{K}^T}{\sqrt{D_e}} + \mathbf{B}\right) \cdot \mathbf{V}, \quad (11)$$

where $\mathbf{A} = \{\mathbf{a}_i\}_{N_{\text{sa}}}$ is a set of self-attention features retaining long-range interactions. Furthermore, the self-attention features \mathbf{A} and input features \mathbf{L} are used to provide the output features $\tilde{\mathbf{A}} = \{\tilde{\mathbf{a}}_i\}_{N_{\text{sa}}} \in \mathbb{R}^{N_{\text{sa}} \times D_{\text{sa}}}$ for the VSAL layer through an MLP:

$$\tilde{\mathbf{A}} = \text{MLP}(\mathbf{A}) + \mathbf{L}. \quad (12)$$

The VSAL layer achieves the goal of $\mathcal{N} \rightarrow \tilde{\mathbf{A}}$ transformation by modeling feature interactions between voxels, thus obtaining outstanding capabilities on global representation.

3) **Encoder:** The architecture of event voxel transformer encoder is presented in Fig. 4. The encoder contains two stages: neighbor embedding and global feature modeling. In the first stage, we stack three MNEL layers and voxel sampling operations to incorporate local information into embedded features hierarchically. This stage also implements set abstraction, which obtains a smaller-size voxel set to reduce the computational cost of self-attention in the next stage. Then the embedded features with corresponding coordinates are fed into two stacked VSAL layers to model global semantics. We concatenate the attention features of each VSAL layer and use an MLP to encode it as the final output $\hat{\mathbf{A}} \in \mathbb{R}^{N_{\text{sa}} \times D_{\text{sa}}}$. Eventually, the encoder can extract semantic information and short-term temporal dynamics by efficient spatiotemporal relation learning.

C. Long-Range Temporal Modeling

In contrast to object classification, which mainly focuses on appearance information, processing an event stream for recognizing human actions requires the model with long-range temporal modeling capabilities. When the duration becomes long, how to model the complex motion patterns on event streams is a challenging topic. Inspired by the advances in video processing methods [35], [36], [40], we introduce a segment modeling strategy to incorporate a long-range temporal structure for event-based action recognition.

Given a long-duration event stream \mathcal{E} , we spilt it into K segments $\{\mathcal{E}_1, \mathcal{E}_2, \dots, \mathcal{E}_K\}$ of equal duration. Each stream segment \mathcal{E}_K is first converted into the event voxel set representation \mathcal{V}_K and then fed into the weight-shared event voxel transformer encoder to learn short-term temporal dynamics $\hat{\mathbf{A}}_K$. We propose the Stream-Segment Temporal Modeling Module (S²TM) to take this sequence $\{\hat{\mathbf{A}}_1, \hat{\mathbf{A}}_2, \dots, \hat{\mathbf{A}}_K\}$ as input for learning the inter-segment dependencies. S²TM maps each segment's feature into a 1D token and uses the transformer encoder layer [32] to aggregate temporal dynamics. In specific, $\hat{\mathbf{A}}_K$ is integrated into a token through a mapping function $\varphi(\cdot) : \mathbb{R}^{N_{\text{sa}} \times D_{\text{sa}}} \rightarrow \mathbb{R}^{D_{\text{sa}}}$. This function concatenates the output from max and average pooling on $\hat{\mathbf{A}}_K$, then encode the feature vector with an MLP. We prepend a learnable classification token $\mathbf{s}_{\text{cls}} \in \mathbb{R}^{D_{\text{sa}}}$ to the front of sequence and add trainable positional embeddings $\mathbf{P}_t \in \mathbb{R}^{(K+1) \times D_{\text{sa}}}$ [32] to tokens for retaining temporal information. Finally, a temporal modeling function processes the sequence to aggregate long-range temporal context. The workflow of S²TM is summarized as follows:

$$\{\hat{\mathbf{s}}_{\text{cls}}, \hat{\mathbf{s}}_1, \dots, \hat{\mathbf{s}}_K\} = h(\{\mathbf{s}_{\text{cls}}, \varphi(\hat{\mathbf{A}}_1), \dots, \varphi(\hat{\mathbf{A}}_K)\} + \mathbf{P}_t), \quad (13)$$

where $\{\hat{s}_{\text{cls}}, \hat{s}_1, \dots, \hat{s}_K\}$ is a sequence of output tokens, and the temporal modeling function $h(\cdot)$ is a transformer encoder layer [32] consisting of multi-head attention layer and feed-forward network. After feature propagation, we use the classification token $\hat{s}_{\text{cls}} \in \mathbb{R}^{D_{\text{sa}}}$ embedded with global temporal context as the final representation for prediction.

D. Network Architecture

As visualized in Fig. 3, the EVSTr model can be applied to both object classification and action recognition tasks. The network architectures for two tasks share a great portion of structures, and we detail them as follows.

1) *Object Classification*: The main challenge of event-based object classification is extracting robust appearance information from short-duration event streams. We convert the entire stream into a single voxel set as input of the classification network. The input is fed into the proposed event voxel transformer encoder to obtain semantic features via spatiotemporal relation learning. We use max and average pooling operations to process the features respectively and concatenate them as a 1D vector. Finally, we use a classification head consisting of three fully connected (FC) layers to transform the global feature vector for categorization. Each FC layer is followed by a BN layer and a ReLU function, except the last one.

2) *Action Recognition*: Unlike object classification which depends on appearance information, a core concern of event-based action recognition is learning temporal dynamics. To retain the long-range temporal structure, we split an event stream into multiple segments for voxel set representations separately and then model the inter-segment temporal dependencies. We utilize the event voxel transformer encoder to extract short-term temporal dynamics from each segment in a weight-shared manner. Then we feed the sequence of segmented features into S²TM to aggregate long-range temporal context. At last, the classification token is processed by the classifier containing a single FC layer to provide the final predicted category.

IV. EXPERIMENTS

In this section, we evaluate the proposed EVSTr model on two event-based recognition tasks, including object classification in Section IV-A and action recognition in IV-B. To complement the lack of real-world event-based action recognition datasets, we present a new benchmark dataset recorded in challenging visual scenarios. Besides, a detailed ablation study is provided in Section IV-C for analyzing the effectiveness of different designs.

A. Object Classification

1) *Dataset*: We validate our method on three representative event-based object classification datasets: N-Caltech101 [41], N-Cars [42] and ASL-DVS [15]. N-Caltech101 is converted from the image dataset Caltech101 using a moving event camera to record images on a monitor. It contains 8,246 samples with the time duration of 300 ms, divided into 101 categories. N-Cars and ASL-DVS are recorded by event cameras in the real-world environment. N-Cars comprises

TABLE I
ACCURACY OF MODELS FOR OBJECT CLASSIFICATION

Method	Type [†]	N-Caltech101	N-Cars	ASL-DVS
Pre-trained on ImageNet				
EST [4]	F	0.837	0.925	0.991
M-LSTM [5]	F	0.857	0.957	0.992
MVF-Net [8]	F	0.871	0.968	0.996
Without Pre-training				
EST [4]	F	0.753	0.919	0.979
M-LSTM [5]	F	0.738	0.927	0.980
MVF-Net [8]	F	0.687	0.927	0.971
AsyNet [6]	F	0.745	0.944	-
RG-CNNs [15]	P	0.657	0.914	0.901
EvS-S [9]	P	0.761	0.931	-
EV-VGCNN [10]	P	0.748	0.953	0.983
AEGNN [19]	P	0.668	0.945	-
VMV-GCN [11]	P	0.778	0.932	0.989
Ours	P	0.797	0.941	0.997

[†]The types ‘‘F’’ and ‘‘P’’ represent frame-based and point-based methods.

24,029 samples in two classes including cars and backgrounds, and each recording lasts 100 ms. ASL-DVS provides 100,800 samples of hand-shaped letters, each sample lasts 100ms, and there are 24 categories. We train our model separately on each training set and evaluate the performance on their testing sets. For N-Caltech101 and ASL-DVS without official splitting, we follow the settings in [10], [15] to randomly select 20% data for testing, and the rest is used for training.

2) Implementation Details:

Representation. The entire event stream is converted into the event voxel set representation (Section III-A) as input of our model. We fix the compensation coefficient T as 4 for all datasets. Considering the different spatiotemporal sizes of the datasets, we set the size (H_v, W_v, T_v) of event voxels as follows: (5, 5, 1) for N-Cars; (10, 10, 1) for N-Caltech101 and ASL-DVS. We set the number N_v of input voxels as: 512 for N-Cars and ASL-DVS; 1024 for N-Caltech101. Moreover, the value D_f of MLP for voxel feature encoding is fixed as 32 in all experiments.

Network Details. The architecture of object classification network is detailed in Section III-D. In the event voxel transformer encoder, we set the output dimensions D_{out} to 64, 64, and 128 for three MNEL layers respectively. The total number N_n of nearest neighbors is 24 when aggregating local features, and the downsampling rate U of voxel sampling operations is 0.75. For two stacked VSAL layers, we set the value of D_{sa} as 128. In the classification head, the output dimensions of three FC layers are 512, 256 and the number of categories. When training, we add dropout layers with a probability of 0.5 after the first two FC layers to avoid overfitting.

Training Settings. The proposed EVSTr model is implemented using PyTorch on a single NVIDIA RTX 3090 GPU. We train the object classification network from scratch for 250 epochs by optimizing the cross-entropy loss using the SGD optimizer with a momentum of 0.9. The batch size is 32 for all datasets. We schedule the learning rate from 3e-2 to 1e-6 with cosine annealing.

3) *Results*: As listed in Table I, we report the accuracy of our

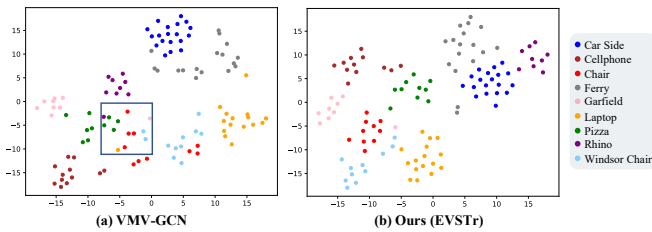


Fig. 5. The t-SNE visualization of feature representations from VMV-GCN and the proposed EVSTr on the N-Caltech101 dataset. Best viewed by zooming in.

model and state-of-the-art methods on three event-based object classification datasets. To conduct a comprehensive analysis, both point-based [9]–[11], [15], [19] and frame-based [4]–[6], [8] methods are our comparison models. For these frame-based methods (i.e., EST [4], M-LSTM [5] and MVF-Net [8]) using pre-trained weights on ImageNet [21], we also report their performance by training from scratch for a fair comparison, since the point-based family cannot be pre-trained on large-scale image datasets.

Compared to point-based peers, our model outperforms state-of-the-art methods and gains a notable improvement (1.9% increase) than the second place on the challenging N-Caltech101 dataset, revealing the effectiveness of our proposed EVSTr. As shown in Fig. 5, we further provide the visualization of feature representations learned by VMV-GCN [11] and ours on the testing samples of N-Caltech101 using t-SNE [43]. The visualization intuitively shows our model learns more discriminative spatiotemporal representations because several confusing samples are not distinguished well using the previous state-of-the-art method VMV-GCN, such as the region highlighted in a bounding box. Both experimental results and feature visualization prove the outstanding representation capabilities of EVSTr, and we attribute the improvement to two key strategies in our model. (i) The MNEL layer attentively embeds multi-scale neighbor information to a local representations for each event voxel. The multi-scale attentive aggregation fully explores the relationship between neighboring voxels and thus can extract discriminative features. (ii) The VSAL layers exploit the long-range dependencies between voxels by feature interactions, allowing us to learn a better global representation than other methods.

Compared to dense frame-based methods using pre-trained models, our method still obtains a competitive performance on ASL-DVS and N-Cars without utilizing prior knowledge from standard images. When training them from scratch for fair competition, the proposed EVSTr achieves higher accuracy than them on all datasets. Besides, our model outperforms the sparse frame-based method AsyNet [6] while keeping lower model complexity. A detailed comparison of model complexity is presented in the following part.

4) *Complexity Analysis*: Table II illustrates the model complexity of different methods on object classification. We evaluate the model complexity comprehensively by three metrics: the number of trainable parameters, the number of multiply-accumulate operations (MACs), and average inference

TABLE II
MODEL COMPLEXITY OF DIFFERENT METHODS ON OBJECT CLASSIFICATION

Method	Type	Params [†]	MACs [†]	Runtime [‡] (ms)
EST [4]	F	21.38M	4.28G	6.41
M-LSTM [5]	F	21.43M	4.82G	10.89
MVF-Net [8]	F	33.62M	5.62G	10.09
AsyNet [6]	F	3.70M	-	-
RG-CNNs [15]	P	19.46M	0.79G	-
EV-VGCNN [10]	P	0.84M	0.70G	7.12
AEGNN [19]	P	20.4M	-	-
VMV-GCN [11]	P	0.86M	1.30G	6.27
Ours	P	0.93M	0.34G	6.62

[†]We report the number of parameters and MACs on N-Caltech101. [‡]The average runtime is during inference on N-Cars.

TABLE III
STATISTICS OF EVENT-BASED ACTION RECOGNITION DATASETS RECORDED IN THE REAL-WORLD ENVIRONMENT

Dataset	Instance	Class	Duration (s)	Modality*	CM [†]	LLI [‡]
DvsGesture [13]	1,342	11	≈ 6.0	E	×	×
DailyAction [16]	1,440	12	1.1 ~ 5.8	E	×	×
NeuroHAR	1,584	18	0.9 ~ 5.7	E, R, D	✓	✓

*E, R, and D denote event, RGB, and depth modalities, respectively. [†]CM denotes camera motion. [‡]LLI denotes low-light illumination.

time. Specifically, we report the number of parameters and MACs on N-Caltech101. Our model achieves the best accuracy on N-Caltech101 while keeping a very low computational complexity (only 0.34G MACs), suggesting the high efficiency of EVSTr in event-based representation learning. We further measure the average inference time of our model on the N-Cars dataset using a workstation (CPU: Intel Core i7, GPU: NVIDIA RTX 3090, RAM: 64GB). Our method needs 6.62 ms to recognize a sample equivalent to a throughput of 151 instances per second, showing the practical potential of EVSTr in high-speed scenarios.

B. Action Recognition

1) *Dataset*: Existing real-world event-based action recognition datasets, such as DVS128 Gesture (DvsGesture) [13] and DailyAction-DVS (DailyAction) [16], are collected in relatively simple visual scenarios. They are recorded by static cameras in sufficient illumination, lacking dynamic backgrounds and low-light challenges. We alleviate the limitations by presenting the Neuromorphic Human Action Recognition dataset (NeuroHAR) recorded in more challenging scenarios, such as low-light illumination and camera motion. The statistics of existing datasets with real event data and our proposed NeuroHAR are listed in Table III.

NeuroHAR Dataset Collection. The recording system consists of an event camera (iniLabs DAVIS 240C [3]) and a RGB-D camera (Intel RealSense D435), as shown in Fig. 6 (a). We synchronize the time of two vision sensors to align the timestamps of event streams and RGB & depth video frames. The NeuroHAR dataset comprises 1,584 instances with 3 modalities of 18 daily human actions, collected from 22 subjects under 2 camera states and 2 illumination conditions.

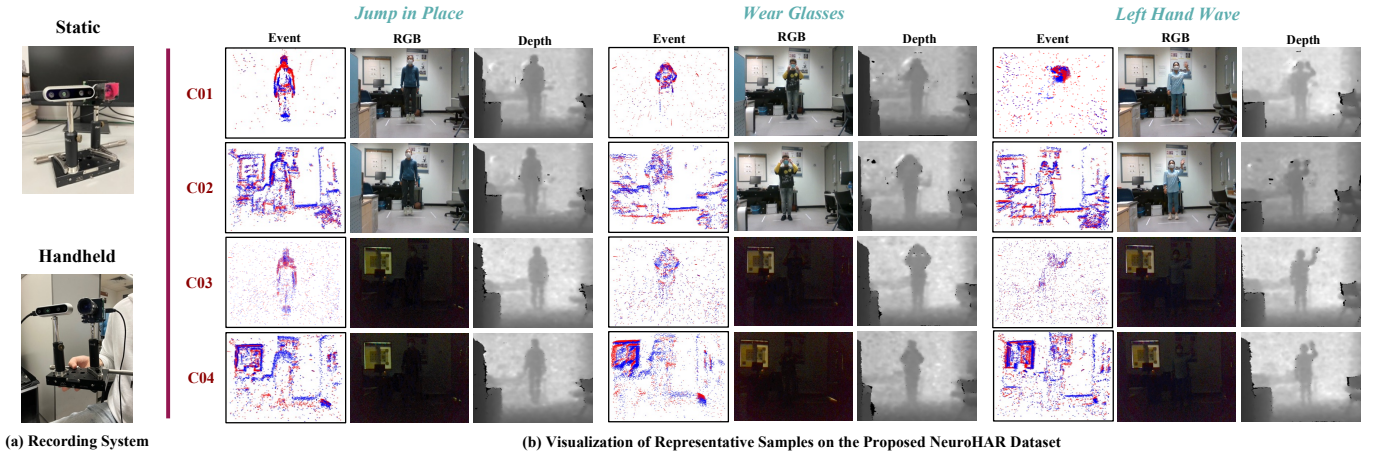


Fig. 6. (a) Recording system. The system consists of an event camera and a RGB-D camera. (b) Visualization of representative samples on the proposed NeuroHAR dataset. Row C01 to C04 represent 4 different recording conditions. C01: normal light illumination and static cameras. C02: normal light illumination and moving cameras. C03: low-light illumination and static cameras. C04: low-light illumination and moving cameras. Best viewed by zooming in.

The duration of each recording lasts from 0.9 to 5.7 seconds. Some representative samples of NeuroHAR are visualized in Fig. 6 (b). As a supplement to recording with static cameras, we preserve the background information in the motion scene by hand-held mobile recording (50% of each category), making the dataset more suitable for practical applications. Besides, we record human actions in normal light and low-light illumination conditions (50% of each category in low-light) to take advantage of the event camera’s high dynamic range. Each subject performs 18-class daily actions in different recording conditions, and the categories of NeuroHAR are: *stand*, *sit down*, *walk*, *run*, *jump forward*, *pick up*, *wear glasses*, *take off glasses*, *hand clap*, *throw*, *left hand wave*, *right hand wave*, *left kick*, *right kick*, *jumping jacks*, *answer the call*, *jump in place* and *carry schoolbag*. These categories contain body movements, human-object interaction (e.g., *carry schoolbag*) and potentially abnormal behavior (e.g., *right kick*), gaining more practical significance. In addition, NeuroHAR provides the recordings with 3 visual modalities including event, RGB and depth, which can be also used for multi-modal action recognition with events and video frames. To evaluate the recognition performance on NeuroHAR, the splitting strategy of the training and testing sets is: 16 subjects are designated as the training set, and the remaining 6 subjects are reserved for testing. NeuroHAR will be available upon acceptance¹.

Pre-Processing. We evaluate the proposed method on three action recognition datasets, including DvsGesture, DailyAction, and newly presented NeuroHAR (only using the event modality). For DvsGesture, we adopt the pre-processing in [11], [14] to cut a 800 ms clip from the entire event stream as input. For other two datasets, the entire event stream is fed into EVSTr for training and inference. EVSTr is trained separately on each training set and evaluated on their testing sets. For DailyAction without a training/testing splitting approach, we follow the settings in [16] to randomly select 20% data for testing, and the remaining samples are used for training.

2) Implementation Details:

¹<https://github.com/bochenxie/NeuroHAR>

Representation. As detailed in Section III-C, an effective segment modeling strategy is introduced to fit the long-range temporal structure of event streams for action recognition. We split an entire event stream into multiple segments for voxel set representations individually: $K = 4$ for DvsGesture and DailyAction; $K = 6$ for more challenging NeuroHAR. For each stream segment, the compensation coefficient T is fixed as 8 in all datasets. When generating the event voxel set per segment, we set the size of event voxels as follows: (5, 5, 1) for DvsGesture and DailyAction; (10, 10, 1) for NeuroHAR. And we set the number N_v of input voxels per segment as: 512 for DvsGesture; 1024 for NeuroHAR and DailyAction. The dimension of voxel feature encoding is also 32.

Network Details. The architecture of action recognition network is illustrated in Fig. 3. The model applied to action recognition and object classification keeps the same settings of event voxel transformer encoder, which are detailed in Section IV-A. We utilize the proposed encoder to extract per-segment features and aggregate them into a final representation by S²TM for recognition. In the S²TM module, the output dimension of mapping function is 512. A shallow transformer encoder layer [32] is used for temporal modeling with the settings: 1-layer depth, 8 heads, 64 for the size of linear transformations in the multi-head attention layer, and 1024 for the dimension of hidden layer in the feed-forward network. The classification head is a single FC layer for predicting action categories.

Training Settings. We train the action recognition network for 300 epochs by optimizing the cross-entropy loss using the SGD optimizer with the batch size of 16. Also, the cosine annealing strategy is used to adjust the learning rate from $1e-2$ to $1e-7$.

3) Results: We compare our model with state-of-the-art point-based and frame-based methods on event-based action recognition. Motion-based SNN (MotionSNN) [16] and graph-based VMV-GCN are selected as representative point-based methods. The experimental results are obtained by their default settings. Moreover, we re-implement several powerful video

TABLE IV
ACCURACY OF MODELS FOR ACTION RECOGNITION

Method	Type	DvsGesture	DailyAction	NeuroHAR
Pre-trained on Kinetics-400				
I3D [†] [44]	F	0.983	0.962	0.854
TANet [†] [45]	F	0.973	0.965	0.866
TimeSformer [34]	F	0.967	0.950	0.828
Without Pre-training				
I3D [‡] [44]	F	0.951	0.909	0.738
TANet [‡] [45]	F	0.974	0.963	0.857
TimeSformer [34]	F	0.917	0.906	0.613
MotionSNN [16]	P	0.927	0.903	-
VMV-GCN [11]	P	0.975	0.941	0.803
Ours	P	0.986	0.996	0.894

[†]The model uses ResNet-50 as the backbone.

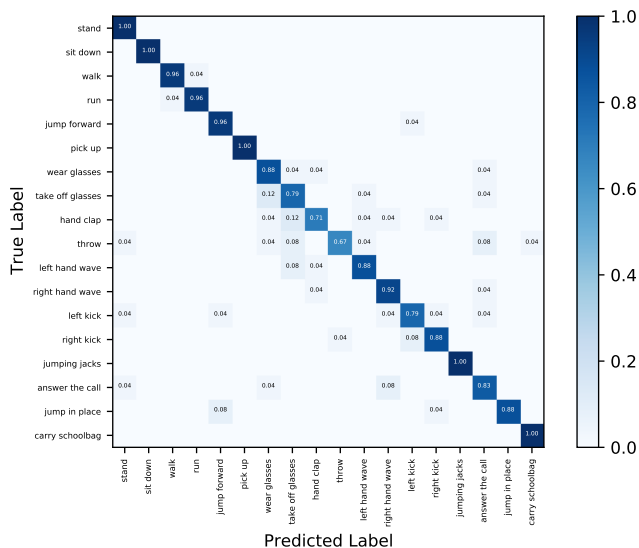


Fig. 7. Confusion matrix of the proposed EVSTr model on the testing set of NeuroHAR. Best viewed by zooming in.

classification models on event-based datasets as frame-based counterparts, such as 3D CNN-based I3D [44], 2D CNN-based TANet [45] and transformer-based TimeSformer [34]. For I3D and TANet, we use ResNet-50 [46] as the backbone. Following the pre-processing approach in [15], we construct an independent 3-channel frame by [25] to integrate events within 1/30 s and densely sample 16 event frames as input of frame-based models. We present their results with and without Kinetics-400 [44] pre-training on benchmark datasets.

We report the recognition performance of EVSTr and state-of-the-art methods in Table IV. The experimental results show that our proposed method obtains the best performance on all testing sets and outperforms the state-of-the-art by a large margin. Excitedly, our model performs better than these frame-based methods pre-trained on the large-scale video dataset Kinetics-400, such as 3.1% improvement on DailyAction and 2.8% improvement on NeuroHAR compared to the second place TANet. This indicates that our proposed method can effectively learn representative temporal dynamics and motion patterns from long-duration event streams. The notable improvement can be attributed to the effective design of the

TABLE V
MODEL COMPLEXITY OF DIFFERENT MODELS FOR ACTION RECOGNITION ON DAILYACTION

Method	Type	Params	MACs	Throughput [†] (ins./s)
I3D [44]	F	49.19M	59.28G	34
TANet [45]	F	24.80M	65.94G	32
TimeSformer [34]	F	121.27M	379.70G	23
VMV-GCN [11]	P	0.84M	0.33G	99
Ours	P	2.88M	1.38G	41

[†]The unit of throughput is the number of processed instances per second when inferring.

TABLE VI
EFFECTIVENESS OF DIFFERENT DESIGNS IN MNEL

Variants	MSE [†]	AFA [‡]	N-Caltech101	DailyAction
A	×	×	0.765	0.986
B	✓	×	0.774	0.990
C	✓	✓	0.797	0.996

[†]MSE denotes multi-scale embedding in the neighborhood space. [‡]AFA denotes attentive feature aggregation for neighboring voxels.

model. (i) The event voxel transformer encoder hierarchically exploits the spatiotemporal relationship between voxels to extract short-term temporal dynamics within a stream segment. (ii) The introduced segment modeling strategy endows EVSTr with long-range temporal learning capabilities, which significantly improves recognition accuracy over others. Furthermore, the confusion matrix of our model on the newly proposed NeuroHAR dataset is shown in Fig. 7, where the EVSTr model distinguishes most categories clearly. Even so, there is still some room for improvement, suggesting NeuroHAR as a challenging dataset.

4) *Complexity Analysis*: The model complexity of different action recognition methods on the DailyAction dataset is summarized in Table V, which includes the number of trainable parameters, the number of MACs and throughput (i.e., the number of processed instances per second when inferring). VMV-GCN has the lowest computational complexity and maximum throughput among all methods by processing short-duration clips from event instances, but its recognition performance is much lower than ours. Compared to frame-based methods with comparable accuracy, our model demonstrates leadership in model complexity since the lightweight EVSTr model takes sparse voxel-wise representations as input and thus benefits from the less redundant computation.

C. Ablation Study

In this subsection, we conduct ablation studies to verify the effectiveness of core design strategies in our proposed model.

1) *Feature Aggregation Strategies in MNEL*: Ablations of the multi-scale attentive aggregation in MNEL on object classification (N-Caltech101) and action recognition (DailyAction) are reported in Table VI. There are several variants representing different feature aggregation strategies. Variant A is a baseline strategy directly using max pooling to aggregate single-scale features in the neighborhood space. Based on this, variant B aggregates neighbor information separately at

TABLE VII
COMPARISON OF DIFFERENT POSITIONAL ENCODING METHODS IN VSAL

Variants	APE [†]	RPB [‡]	N-Caltech101	DailyAction
1	×	×	0.755	0.958
2	✓	×	0.772	0.983
3	×	✓	0.761	0.976
4	✓	✓	0.797	0.996

[†]APE denotes absolute positional encoding. [‡]RPB denotes relative position bias.

TABLE VIII
EFFECTIVENESS OF SEGMENT MODELING STRATEGY ON ACTION RECOGNITION

S ² TM	Temporal Modeling	DvsGesture	DailyAction	NeuroHAR
×	-	0.976	0.954	0.809
✓	Average Pooling	0.979	0.993	0.840
	LSTM	0.976	0.983	0.884
	Self-attention	0.986	0.996	0.894

multiple scales and then sums them together to obtain multi-scale features. It achieves slight improvements on both tasks, demonstrating that the multi-scale approach enhances local feature extraction. Nevertheless, searching and aggregating neighbor features only considering the positional relationship may fail to obtain robust local features. To this end, our proposed MNEL layer (variant C) exploits both positional and semantic relations to attentively aggregate neighbor features instead of max pooling in variant B. The multi-scale attention aggregation strategy significantly improves the recognition accuracy over the baseline, suggesting the importance of fully modeling relations and the superiority of attentive aggregation.

2) *Positional Encoding in VSAL*: Table VII compares different positional encoding approaches in VSAL on object classification and action recognition. Without any positional embeddings, variant 1 only uses the original self-attention operator lacking the positional information, thus limiting its global modeling capabilities. Introducing the absolute positional embeddings (variant 2) or relative position bias (variant 3) individually improves recognition accuracy slightly on both tasks. Interestingly, after adding the relative position bias individually, variant 3 achieves a more considerable gain in action recognition than object classification, which indicates that relative position may express the positional relationship between voxels better in non-fixed motion patterns. When using absolute-relative positional encoding, variant 4 (our model) achieves the best recognition performance, indicating that the proposed positional encoding strategy effectively assists self-attention in computing semantic affinities between voxels.

3) *Effectiveness of Segment Modeling Strategy on Action Recognition*: We conduct an ablation study to verify the effectiveness of segment modeling strategy and discuss its performance with different temporal modeling functions, as listed in Table VIII. After using S²TM to perform segment modeling, the recognition performance of our model improves significantly, demonstrating that this strategy enables EVSTr incorporates a long-range temporal structure. Then we adopt three mainstream temporal modeling approaches in S²TM for experiments, including average pooling, long short-term mem-

ory (LSTM), and self-attention. Our model achieves competitive accuracy compared to the state-of-the-art regardless of the approach used. On the relatively simple datasets DvsGesture and DailyAction, the basic average pooling even outperforms advanced LSTM. However, on NeuroHAR with more complex temporal dynamics, the learning-based functions, self-attention and LSTM, will lead to better recognition performance. This fact suggests that: (i) Adaptive temporal modeling based on self-attention enables efficient modeling of complex temporal dynamics. (ii) The proposed NeuroHAR is a challenging dataset that can comprehensively evaluate the performance of event-based models. Therefore, we default to the transformer encoder layer as a temporal modeling function in S²TM.

V. CONCLUSION

This work introduces a novel attention-aware model (EVSTr) for spatiotemporal representation learning on event streams. It takes event voxel sets as input to fit the sparsity of event data and hierarchically explores the relationship between voxels. The proposed event voxel transformer encoder is endowed to extract local and global spatiotemporal features by two well-designed components, including MNEL and VSAL. To model the long-range temporal structure for action recognition, a segment modeling strategy combined with S²TM is introduced to learn temporal dynamics from a sequence of segmented voxel sets. Comprehensive experiments on object classification and action recognition show that EVSTr achieves significant accuracy gains and impressively low model complexity compared to state-of-the-art methods. Moreover, we present a new event-based action recognition dataset (NeuroHAR) with multiple modalities recorded in challenging visual scenarios, allowing comprehensive evaluation for event-based models. In the future, we plan to design a multi-modal model for human action recognition with events and video frames to unlock the complementary potential of event and traditional cameras.

REFERENCES

- [1] P. Lichtsteiner, C. Posch, and T. Delbruck, "A 128 × 128 120 db 15 μ s latency asynchronous temporal contrast vision sensor," *IEEE J. Solid-State Circuits*, vol. 43, no. 2, pp. 566–576, Feb. 2008.
- [2] C. Posch, D. Matolin, and R. Wohlgenannt, "A QVGA 143 db dynamic range frame-free PWM image sensor with lossless pixel-level video compression and time-domain CDS," *IEEE J. Solid-State Circuits*, vol. 46, no. 1, pp. 259–275, Jan. 2010.
- [3] C. Brandli, R. Berner, M. Yang, S.-C. Liu, and T. Delbruck, "A 240 × 180 130 db 3 μ s latency global shutter spatiotemporal vision sensor," *IEEE J. Solid-State Circuits*, vol. 49, no. 10, pp. 2333–2341, Oct. 2014.
- [4] D. Gehrig, A. Loquercio, K. G. Derpanis, and D. Scaramuzza, "End-to-end learning of representations for asynchronous event-based data," in *Proc. IEEE/CVF Int. Conf. Comput. Vis.*, 2019, pp. 5633–5643.
- [5] M. Cannici, M. Ciccone, A. Romanoni, and M. Matteucci, "A differentiable recurrent surface for asynchronous event-based data," in *Proc. Eur. Conf. Comput. Vis.*, 2020, pp. 136–152.
- [6] N. Messikommer, D. Gehrig, A. Loquercio, and D. Scaramuzza, "Event-based asynchronous sparse convolutional networks," in *Proc. Eur. Conf. Comput. Vis.*, 2020, pp. 415–431.
- [7] Y. Deng, Y. Li, and H. Chen, "AMAE: Adaptive motion-agnostic encoder for event-based object classification," *IEEE Robot. Autom. Lett.*, vol. 5, no. 3, pp. 4596–4603, Jul. 2020.
- [8] Y. Deng, H. Chen, and Y. Li, "MVF-Net: A multi-view fusion network for event-based object classification," *IEEE Trans. Circuits Syst. Video Technol.*, vol. 32, no. 12, pp. 8275–8284, Dec. 2022.

- [9] Y. Li, H. Zhou, B. Yang, Y. Zhang, Z. Cui, H. Bao, and G. Zhang, "Graph-based asynchronous event processing for rapid object recognition," in *Proc. IEEE/CVF Int. Conf. Comput. Vis.*, 2021, pp. 934–943.
- [10] Y. Deng, H. Chen, H. Liu, and Y. Li, "A voxel graph CNN for object classification with event cameras," in *Proc. IEEE/CVF Conf. Comput. Vis. Pattern Recognit.*, 2022, pp. 1172–1181.
- [11] B. Xie, Y. Deng, Z. Shao, H. Liu, and Y. Li, "VMV-GCN: Volumetric multi-view based graph CNN for event stream classification," *IEEE Robot. Autom. Lett.*, vol. 7, no. 2, pp. 1976–1983, Apr. 2022.
- [12] Z. Wang, Y. Hu, and S.-C. Liu, "Exploiting spatial sparsity for event cameras with visual transformers," in *Proc. IEEE Conf. Image Process.*, 2022, pp. 411–415.
- [13] A. Amir *et al.*, "A low power, fully event-based gesture recognition system," in *Proc. IEEE/CVF Conf. Comput. Vis. Pattern Recognit.*, 2017, pp. 7388–7397.
- [14] Q. Wang, Y. Zhang, J. Yuan, and Y. Lu, "Space-time event clouds for gesture recognition: From RGB cameras to event cameras," in *Proc. IEEE Winter Conf. Appl. Comput. Vis.*, 2019, pp. 1826–1835.
- [15] Y. Bi, A. Chadha, A. Abbas, E. Bourtsoulatzé, and Y. Andreopoulos, "Graph-based spatio-temporal feature learning for neuromorphic vision sensing," *IEEE Trans. Image Process.*, vol. 29, pp. 9084–9098, Sep. 2020.
- [16] Q. Liu, D. Xing, H. Tang, D. Ma, and G. Pan, "Event-based action recognition using motion information and spiking neural networks," in *Proc. 30th Int. Joint Conf. Artif. Intell.*, 2021, pp. 1743–1749.
- [17] E. Perot, P. de Tournemire, D. Nitti, J. Masci, and A. Sironi, "Learning to detect objects with a 1 megapixel event camera," in *Proc. Adv. Neural Inf. Process. Syst.*, vol. 33, 2020, pp. 16 639–16 652.
- [18] J. Li *et al.*, "Asynchronous spatio-temporal memory network for continuous event-based object detection," *IEEE Trans. Image Process.*, vol. 31, pp. 2975–2987, Apr. 2022.
- [19] S. Schaefer, D. Gehrig, and D. Scaramuzza, "AEGNN: Asynchronous event-based graph neural networks," in *Proc. IEEE/CVF Conf. Comput. Vis. Pattern Recognit.*, 2022, pp. 12 371–12 381.
- [20] G. Gallego *et al.*, "Event-based vision: A survey," *IEEE Trans. Pattern Anal. Mach. Intell.*, vol. 44, no. 1, p. 154–180, Jan. 2022.
- [21] J. Deng, W. Dong, R. Socher, L.-J. Li, K. Li, and L. Fei-Fei, "ImageNet: A large-scale hierarchical image database," in *Proc. IEEE/CVF Conf. Comput. Vis. Pattern Recognit.*, 2009, pp. 248–255.
- [22] G. Orchard, C. Meyer, R. Etienne-Cummings, C. Posch, N. Thakor, and R. Benosman, "HFirst: A temporal approach to object recognition," *IEEE Trans. Pattern Anal. Mach. Intell.*, vol. 37, no. 10, pp. 2028–2040, Oct. 2015.
- [23] Y. Sekikawa, K. Hara, and H. Saito, "EventNet: Asynchronous recursive event processing," in *Proc. IEEE/CVF Conf. Comput. Vis. Pattern Recognit.*, 2019, pp. 3887–3896.
- [24] A. I. Maqueda, A. Loquercio, G. Gallego, N. García, and D. Scaramuzza, "Event-based vision meets deep learning on steering prediction for self-driving cars," in *Proc. IEEE Conf. Comput. Vis. Pattern Recognit.*, 2018, pp. 5419–5427.
- [25] A. Z. Zhu, L. Yuan, K. Chaney, and K. Daniilidis, "Unsupervised event-based optical flow using motion compensation," in *Proc. Eur. Conf. Comput. Vis.*, 2018, pp. 711–714.
- [26] Y. Deng, H. Chen, H. Chen, and Y. Li, "Learning from images: A distillation learning framework for event cameras," *IEEE Trans. Image Process.*, vol. 30, pp. 4919–4931, May 2021.
- [27] L. Wang, Y. Chae, S.-H. Yoon, T.-K. Kim, and K.-J. Yoon, "EvDistill: Asynchronous events to end-task learning via bidirectional reconstruction-guided cross-modal knowledge distillation," in *Proc. IEEE/CVF Conf. Comput. Vis. Pattern Recognit.*, 2021, pp. 608–619.
- [28] N. Messikommer, D. Gehrig, M. Gehrig, and D. Scaramuzza, "Bridging the gap between events and frames through unsupervised domain adaptation," *IEEE Robot. Autom. Lett.*, vol. 7, no. 2, pp. 3515–3522, Jan. 2022.
- [29] C. R. Qi, H. Su, K. Mo, and L. J. Guibas, "PointNet: Deep learning on point sets for 3D classification and segmentation," in *Proc. IEEE Conf. Comput. Vis. Pattern Recognit.*, 2017, pp. 652–660.
- [30] C. R. Qi, L. Yi, H. Su, and L. J. Guibas, "PointNet++: Deep hierarchical feature learning on point sets in a metric space," in *Proc. Adv. Neural Inf. Process. Syst.*, vol. 30, 2017, pp. 5099–5108.
- [31] A. Vaswani *et al.*, "Attention is all you need," in *Proc. Adv. Neural Inf. Process. Syst.*, vol. 30, 2017, pp. 6000–6010.
- [32] A. *et al.* Dosovitskiy, "An image is worth 16x16 words: Transformers for image recognition at scale," in *Proc. Int. Conf. Learn. Representations*, 2021, pp. 1–21.
- [33] Z. Liu *et al.*, "Swin transformer: Hierarchical vision transformer using shifted windows," in *Proc. IEEE/CVF Int. Conf. Comput. Vis.*, 2021, pp. 10 012–10 022.
- [34] G. Bertasius, H. Wang, and L. Torresani, "Is space-time attention all you need for video understanding?" in *Proc. Int. Conf. on Mach. Learn.*, vol. 2, no. 3, 2021, p. 4.
- [35] A. Arnab *et al.*, "ViViT: A video vision transformer," in *Proc. IEEE/CVF Int. Conf. Comput. Vis.*, 2021, pp. 6836–6846.
- [36] D. Neimark, O. Bar, M. Zohar, and D. Asselmann, "Video transformer network," in *Proc. IEEE/CVF Int. Conf. Comput. Vis. Workshops*, 2021, pp. 3163–3172.
- [37] M.-H. Guo *et al.*, "PCT: Point cloud transformer," *Comput. Vis. Media*, vol. 7, pp. 187–199, 2021.
- [38] H. Zhao, L. Jiang, J. Jia, P. H. Torr, and V. Koltun, "Point transformer," in *Proc. IEEE/CVF Int. Conf. Comput. Vis.*, 2021, pp. 16 259–16 268.
- [39] Y. Tian and J. Andrade-Cetto, "Event transformer FlowNet for optical flow estimation," in *Proc. 33rd Brit. Mach. Vis. Conf.*, 2022, p. 577.
- [40] L. Wang *et al.*, "Temporal segment networks for action recognition in videos," *IEEE Trans. Pattern Anal. Mach. Intell.*, vol. 41, no. 11, pp. 2740–2755, Sep. 2018.
- [41] G. Orchard, A. Jayawant, G. K. Cohen, and N. Thakor, "Converting static image datasets to spiking neuromorphic datasets using saccades," *Front. Neurosci.*, vol. 9, p. 437, 2015.
- [42] A. Sironi, M. Brambilla, N. Bourdis, X. Lagorce, and R. Benosman, "HATS: Histograms of averaged time surfaces for robust event-based object classification," in *Proc. IEEE/CVF Conf. Comput. Vis. Pattern Recognit.*, 2018, pp. 1731–1740.
- [43] L. Van der Maaten and G. Hinton, "Visualizing data using t-SNE," *Journal of Mach. Learn. Res.*, vol. 9, no. 11, 2008.
- [44] J. Carreira and A. Zisserman, "Quo vadis, action recognition? A new model and the kinetics dataset," in *Proc. IEEE/CVF Conf. Comput. Vis. Pattern Recognit.*, 2017, pp. 6299–6308.
- [45] Z. Liu, L. Wang, W. Wu, C. Qian, and T. Lu, "TAM: Temporal adaptive module for video recognition," in *Proc. IEEE/CVF Int. Conf. Comput. Vis.*, 2021, pp. 13 708–13 718.
- [46] K. He, X. Zhang, S. Ren, and J. Sun, "Deep residual learning for image recognition," in *Proc. IEEE/CVF Conf. Comput. Vis. Pattern Recognit.*, 2016, pp. 770–778.